

Technical report 06-022

# **A comparison of filter configurations for freeway traffic state estimation\***

A. Hegyi, D. Girimonte, R. Babuška, and B. De Schutter

*If you want to cite this report, please use the following reference instead:*

A. Hegyi, D. Girimonte, R. Babuška, and B. De Schutter, “A comparison of filter configurations for freeway traffic state estimation,” *Proceedings of the 2006 IEEE Intelligent Transportation Systems Conference (ITSC 2006)*, Toronto, Canada, pp. 1029–1034, Sept. 2006.

Delft Center for Systems and Control  
Delft University of Technology  
Mekelweg 2, 2628 CD Delft  
The Netherlands  
phone: +31-15-278.51.19 (secretary)  
fax: +31-15-278.66.79  
URL: <http://www.dcsc.tudelft.nl>

---

\*This report can also be downloaded via [http://pub.deschutter.info/abs/06\\_022.html](http://pub.deschutter.info/abs/06_022.html)

# A comparison of filter configurations for freeway traffic state estimation

A. Hegyi, D. Girimonte, R. Babuška, B. De Schutter

**Abstract**—We present a comparison for several filter configurations for freeway traffic state estimation. Since the environmental conditions on a freeway may change over time (e.g., changing weather conditions), parameter estimation is also considered. We compare the performance of the extended Kalman filter and the unscented Kalman filter for state estimation, parameter estimation, joint estimation and dual estimation. Furthermore, the performance is evaluated for different detector configurations.

The main conclusions from the simulations are that (1) the performance of the extended Kalman filter and the unscented Kalman filter is comparable, (2) joint filtering performs significantly better than dual filtering, and (3) a larger number of detectors results in better state estimation, but has no significant influence on the parameter estimation error.

## I. INTRODUCTION

Dynamic traffic control offers possibilities to avoid traffic jams on freeways by making better use of the available infrastructure. Measures such as ramp metering, dynamic speed limits and route guidance increase the efficiency, reliability and safety of traffic flows. The choice of the actual control actions is typically based on the current traffic state. However, the traffic state is usually not available or not directly measured everywhere in the traffic network (e.g., density is in general not measured). The data may also be corrupted or be unreliable because of malfunctioning or noisy sensors (magnetic loops or cameras).

In other application areas the state of a dynamical system is typically estimated by the Kalman filter (KF) [1] or one of its variants, such as the extended Kalman filter (EKF) [2], the unscented Kalman filter (UKF) [3], [4] or by particle filters (PF) [5]. In the selection of the appropriate filter type and the filter configuration for a given problem several design choices are involved. The goal of this paper is to investigate some of these choices, namely the selection of an appropriate filter type and configuration, and the influence of detector configurations on the performance.

These different filter configurations can be used to estimate the state of the process, the parameters, or both. When both the state and the parameters are estimated, two common approaches exist, the *joint* filtering approach where both the state and the parameters are considered as the states of an augmented system and “state” estimation is performed for the augmented state, and the *dual* filtering approach where the state and the parameters are estimated in parallel by two separate filters. It has been suggested that dual filtering

has better convergence properties [2]. In simulations we compare the performance of both filters, and conclude that this suggestion is not confirmed for our case.

Another aspect that influences the performance is the availability and the number of outputs (measurement sources). In general, the fewer outputs there are, the worse the estimate of the state. If there are too few outputs then some states may become unobservable, i.e., the measurements do not carry enough information about the state. In this paper, we also investigate the effect of different measurement loop configurations on the performance.

Several filters in several configurations have already been investigated in literature. In [6] an extended study is presented of estimation schemes with the EKF in the joint filtering setting [2], [7]. This approach is evaluated for real traffic data in [8], [9]. In [10] a PF is applied to estimate the traffic state (speed and density) of a 4-segment freeway stretch based on flow and speed measurements at the boundaries of the stretch. A different approach was developed in [11] where a mixture Kalman filter is employed to simultaneously detect the discrete traffic state (free-flow or congested) and track the traffic speed. While in most papers the intended use of the estimated state is control, in [12] queue tail and head tracking and travel time estimation is considered as a service to drivers.

According to recent developments, the UKF is an interesting alternative to the EKF for nonlinear systems, since it has a higher accuracy [3], [4]. Furthermore in all publications mentioned above, the EKF is used in the joint filtering setting in which both the traffic state and the parameters are estimated, while in [2] it is suggested that the dual filtering setting may exhibit better convergence properties.

The contribution of this paper is the comparison of the EKF and UKF for freeway traffic state estimation, parameter estimation, joint and dual estimation, and the evaluation of the performances as a function of the detector configuration.

In the remainder of the paper the different filters will be analyzed with the freeway traffic flow model METANET [13]. The various filters and their possible configurations are discussed in Section II, and the METANET model is explained in detail in Section III. This model is used for the simulations in Section IV, and the results are presented in Section V.

## II. STATE ESTIMATION

In state estimation problems, the state-space representation of the dynamical system is used. This describes the evolution of the system state  $\mathbf{x}_k$  over time, and the measurements  $\mathbf{y}_k$

A. Hegyi, R. Babuška, B. De Schutter are with the Delft Center for Systems and Control, Delft University of Technology, Mekelweg 2, 2628 CD, Delft, The Netherlands. Email: {a.hegyi, r.babuska, b.deschutter}@tudelft.nl

D. Girimonte is with ESA, ESTEC, EUI-ACT, Keplerlaan 1, 2201 AZ Noordwijk, The Netherlands. Email: Daniela.Girimonte@esa.int

as a function of the state<sup>1</sup>:

$$\mathbf{x}_k = \mathbf{f}(\mathbf{x}_{k-1}, \mathbf{w}, \mathbf{v}_{k-1}) \quad (1)$$

$$\mathbf{y}_k = \mathbf{g}(\mathbf{x}_k, \mathbf{w}, \mathbf{n}_k) \quad (2)$$

where  $\mathbf{w}$  are the model parameters,  $\mathbf{v}_k$  is the state noise,  $\mathbf{n}_k$  the measurement noise, and  $k$  the sample step counter. For given parameters  $\mathbf{w}$  these equations define a probability density function (pdf) for the state transition  $p(\mathbf{x}_k|\mathbf{x}_{k-1})$  and for the measurement  $p(\mathbf{y}_k|\mathbf{x}_k)$ .

Since the system and the measurements are stochastic, the exact state cannot be inferred from the measurements, only the pdf of the state  $p(\mathbf{x}_k|\mathbf{y}_{1:k})$  given all measurements  $\mathbf{y}_{1:k}$  from sample step 1 to  $k$  can be determined. So, the goal of the state estimation problem is to determine  $p(\mathbf{x}_k|\mathbf{y}_{1:k})$ . Although it is possible to use Bayes' rule to express this conditional density in terms of the state transition pdf  $p(\mathbf{x}_k|\mathbf{x}_{k-1})$ , and the measurement pdf  $p(\mathbf{y}_k|\mathbf{x}_k)$ , the evaluation of it requires the evaluation of several integrals, which is not possible (analytically) in general [5]. In principle it is possible to evaluate these integrals numerically (which is done, e.g., in approximate grid-based methods where the state space is discretized [5]), but these methods are in most cases very inefficient.

Under certain assumptions the conditional pdf  $p(\mathbf{x}_k|\mathbf{y}_{1:k})$  can be solved (or approximated) by the Kalman filter or its extensions, such as the extended/unscented Kalman filter. Below we give a short overview of the Kalman filter, the extended Kalman filter and the unscented Kalman filter and their corresponding assumptions. Note that there are other filtering methods that are not discussed here.

#### A. Filter types

1) *Kalman filter (KF)*: Given a linear system

$$\mathbf{x}_k = \mathbf{A}\mathbf{x}_{k-1} + \mathbf{v}_{k-1}$$

$$\mathbf{y}_k = \mathbf{C}\mathbf{x}_k + \mathbf{n}_k$$

with known and constant system matrices  $\mathbf{A}$  and  $\mathbf{C}$ . The state noise  $\mathbf{v}_{k-1}$  and measurement noise  $\mathbf{n}_k$  are both assumed to be additive, and assumed to have a zero mean Gaussian distribution. Furthermore independence between noises at different time instants and between the state and measurement noise is assumed:  $\text{cov}\{\mathbf{v}_{k_1}, \mathbf{v}_{k_2}\} = 0$  and  $\text{cov}\{\mathbf{n}_{k_1}, \mathbf{n}_{k_2}\} = 0$  for  $k_1 \neq k_2$ , and  $\text{cov}\{\mathbf{v}_{k_1}, \mathbf{n}_{k_2}\} = 0$  for any  $k_1$  and  $k_2$ .

Under these assumptions the conditional pdf  $p(\mathbf{x}_k|\mathbf{y}_{1:k})$  is also Gaussian, and the Kalman filter expresses analytically the mean and covariance of  $p(\mathbf{x}_k|\mathbf{y}_{1:k})$  [2]. The Kalman filter is guaranteed to converge if the state noise excites all states and the system  $(\mathbf{C}, \mathbf{A})$  is observable [1].

The KF is not suitable for nonlinear systems such as the freeway traffic, so we will not present the equations<sup>2</sup>.

<sup>1</sup>For simplicity, we do not consider inputs that may act on the system. The extension to include inputs is straightforward.

<sup>2</sup>However, the EKF equations reduce to the Kalman filter if the system is linear. The EKF equations are given in Table I.

TABLE I  
THE EXTENDED KALMAN FILTER

<p>I. Initialize the estimate <math>\hat{\mathbf{x}}_k</math> of the state and the covariance <math>\mathbf{P}_{\mathbf{x}_k}</math> of the state with:</p> $\hat{\mathbf{x}}_0 = \mathbf{E}[\mathbf{x}_0],$ $\mathbf{P}_{\mathbf{x}_0} = \mathbf{E}[(\mathbf{x}_0 - \hat{\mathbf{x}}_0)(\mathbf{x}_0 - \hat{\mathbf{x}}_0)^T].$ <p>Evaluate steps II and III below for <math>k = 1, 2, \dots</math></p> <p>II. Time update:</p> $\hat{\mathbf{x}}_k^- = \mathbf{f}(\hat{\mathbf{x}}_{k-1}, \mathbf{w}),$ $\mathbf{P}_{\mathbf{x}_k}^- = \mathbf{A}_{k-1}\mathbf{P}_{\mathbf{x}_{k-1}}\mathbf{A}_{k-1}^T + \mathbf{R}^v,$ <p>where <math>\mathbf{w}</math> is the parameter vector, and <math>\mathbf{R}^v</math> is the covariance of the state noise <math>\mathbf{v}_k</math>.</p> <p>III. Measurement update:</p> $\mathbf{K}_k = \mathbf{P}_{\mathbf{x}_k}^- \mathbf{C}_k^T (\mathbf{C}_k \mathbf{P}_{\mathbf{x}_k}^- \mathbf{C}_k^T + \mathbf{R}^n)^{-1},$ $\hat{\mathbf{x}}_k = \hat{\mathbf{x}}_k^- + \mathbf{K}_k (\mathbf{y}_k - \mathbf{g}(\hat{\mathbf{x}}_k^-, \mathbf{w})),$ $\mathbf{P}_{\mathbf{x}_k} = (\mathbf{I} - \mathbf{K}_k \mathbf{C}_k) \mathbf{P}_{\mathbf{x}_k}^-,$ <p>where</p> $\mathbf{A}_k = \left. \frac{\partial \mathbf{f}(\mathbf{x}, \mathbf{w})}{\partial \mathbf{x}} \right _{\mathbf{x}=\hat{\mathbf{x}}_k}, \quad \mathbf{C}_k = \left. \frac{\partial \mathbf{g}(\mathbf{x}, \mathbf{w})}{\partial \mathbf{x}} \right _{\mathbf{x}=\hat{\mathbf{x}}_k},$ <p>and <math>\mathbf{R}^n</math> is the covariance of the measurement noise <math>\mathbf{n}_k</math>.</p>
--

2) *Extended Kalman filter (EKF)*: The assumptions for the EKF are the same as for the Kalman filter, except that the state and measurement functions may be nonlinear. To solve the filtering problem, the system is linearized at the *estimated* state for each  $k$  [2]. The equations of the EKF are given in Table I.

The extended Kalman filter does not solve the estimation problem exactly, since approximations are involved. First, the system is linearized at the estimated state instead of the real (but unknown) state. Second, by linearization, all pdf's are Gaussian, while the real pdf's passing through the nonlinear system is obviously non-Gaussian. The consequence of these approximations is that convergence cannot be guaranteed.

3) *Unscented Kalman filter (UKF)*: Contrary to the EKF, the UKF does not use a linearization of the system and the noises are not assumed to be Gaussian [3], [4]. To represent the mean and the covariance of the (conditional) state pdf's, so-called sigma points are defined with appropriate weights attached to each point. The sigma points and the weights are chosen such that their weighted mean and covariance approximate the true mean and covariance of the pdf.

The UKF approximates the mean and the covariance of the posterior pdf with second order (Taylor) accuracy. As the EKF operates with first order accuracy, the UKF can be expected to have better performance and convergence properties. Nevertheless, convergence cannot be guaranteed for the UKF.

The equations of the UKF are given in Table II. The main assumption here is that the state pdf can be sufficiently described by its mean and covariance.

#### B. Filter configurations

These filters can be used for state estimation, parameter estimation, or for the simultaneous estimation of the state and the parameters. These require different filter configurations, which are summarized below.

TABLE II  
THE UNSCENTED KALMAN FILTER

<p>I. Initialize with:</p> $\hat{\mathbf{x}}_0 = E[\mathbf{x}_0], \mathbf{P}_0 = E[(\mathbf{x}_0 - \hat{\mathbf{x}}_0)(\mathbf{x}_0 - \hat{\mathbf{x}}_0)^T], \hat{\mathbf{x}}_0^a = E[\mathbf{x}_0^a],$ $\mathbf{P}_0^a = E[(\mathbf{x}_0^a - \hat{\mathbf{x}}_0^a)(\mathbf{x}_0^a - \hat{\mathbf{x}}_0^a)^T] = \text{diag}\{\mathbf{P}_0, \mathbf{P}_v, \mathbf{P}_n\}$ <p>where <math>\mathbf{x}_k^a = [\mathbf{x}_k^T \mathbf{v}_k^T \mathbf{n}_k^T]^T</math> is the augmented state vector.</p> <p>Evaluate steps II, III, and IV below for <math>k = 1, 2, \dots</math></p> <p>II. Calculate sigma points:</p> $\mathcal{X}_{0,k-1}^a = \hat{\mathbf{x}}_{k-1}^a$ $\mathcal{X}_{i,k-1}^a = \hat{\mathbf{x}}_{k-1}^a + (\sqrt{(n_x + \lambda)\mathbf{P}_{k-1}^a})_i, \quad \text{for } i = 1, \dots, n_x$ $\mathcal{X}_{i,k-1}^a = \hat{\mathbf{x}}_{k-1}^a - (\sqrt{(n_x + \lambda)\mathbf{P}_{k-1}^a})_{i-n_x}, \quad \text{for } i = n_x + 1, \dots, 2n_x$ <p>where <math>\mathcal{X}_k^a = [(\mathcal{X}_k^x)^T (\mathcal{X}_k^v)^T (\mathcal{X}_k^n)^T]^T</math> and <math>\sqrt{\mathbf{P}_{k-1}^a}</math> is a Cholesky factor, and the design parameters selected as <math>\lambda = \alpha^2(n_x + \kappa) - n_x</math>, <math>1 \geq \alpha \geq 10^{-4}</math>, <math>\kappa</math> is typically taken to equal <math>3 - n_x</math>, and <math>n_x</math> is the dimension of the augmented state, and <math>(\mathbf{M})_i</math> denotes the <math>i</math>-th column of matrix <math>\mathbf{M}</math>.</p> <p>III. Time update :</p> $\mathcal{X}_{i,k k-1}^x = \mathbf{f}(\mathcal{X}_{i,k-1}^x, \mathcal{X}_{i,k-1}^v),$ $\hat{\mathbf{x}}_{k k-1} = \sum_{i=0}^{2n_x} W_i^{(m)} \mathcal{X}_{i,k k-1}^x,$ $\mathbf{P}_{k k-1} = \sum_{i=0}^{2n_x} W_i^{(c)} [\mathcal{X}_{i,k k-1}^x - \hat{\mathbf{x}}_{k k-1}][\mathcal{X}_{i,k k-1}^x - \hat{\mathbf{x}}_{k k-1}]^T,$ $\mathcal{Y}_{i,k k-1} = \mathbf{g}(\mathcal{X}_{i,k k-1}^x, \mathcal{X}_{i,k-1}^n),$ $\hat{\mathbf{y}}_{k k-1} = \sum_{i=0}^{2n_x} W_i^{(m)} \mathcal{Y}_{i,k k-1}.$ <p>IV. Measurement update:</p> $\mathbf{P}_{\mathbf{y}_k \mathbf{y}_k} = \sum_{i=0}^{2n_x} W_i^{(c)} [\mathcal{Y}_{i,k k-1} - \hat{\mathbf{y}}_{k k-1}][\mathcal{Y}_{i,k k-1} - \hat{\mathbf{y}}_{k k-1}]^T,$ $\mathbf{P}_{\mathbf{x}_k \mathbf{y}_k} = \sum_{i=0}^{2n_x} W_i^{(c)} [\mathcal{X}_{i,k k-1}^x - \hat{\mathbf{x}}_{k k-1}][\mathcal{Y}_{i,k k-1} - \hat{\mathbf{y}}_{k k-1}]^T,$ $\mathcal{K}_k = \mathbf{P}_{\mathbf{x}_k \mathbf{y}_k} \mathbf{P}_{\mathbf{y}_k \mathbf{y}_k}^{-1},$ $\hat{\mathbf{x}}_{k k} = \hat{\mathbf{x}}_{k k-1} + \mathcal{K}_k (\mathbf{y}_k - \hat{\mathbf{y}}_{k k-1}),$ $\mathbf{P}_{k k} = \mathbf{P}_{k k-1} - \mathcal{K}_k \mathbf{P}_{\mathbf{y}_k \mathbf{y}_k} \mathcal{K}_k^T,$ <p>where the weights are: <math>W_0^{(m)} = \lambda/(n_x + \lambda)</math>,  <math>W_0^{(c)} = \lambda/(n_x + \lambda) + (1 - \alpha^2 + \beta)</math>,  <math>W_i^{(m)} = W_i^{(c)} = 1/2(n_x + \lambda)</math>, for <math>i = 1, \dots, 2n_x</math>.</p>
---

1) *State tracking*: The model parameters are assumed to be known. The goal of state tracking is to determine the pdf  $p(\mathbf{x}_k | \mathbf{y}_{1:k})$  for every  $k$ .

2) *Parameter tracking*: The model states and measurements are assumed to be known. The state-space model is formed for the evolution of the model parameters  $\mathbf{x}_{\text{par},k} = \mathbf{w}_k$ , which is often assumed to be a random walk with noise  $\mathbf{v}_{\text{par},k}$ . The measurement is written as a function of the system state  $\mathbf{x}_k$  and the model parameters  $\mathbf{x}_{\text{par},k}$ , and a “state tracking” filter is run for  $\mathbf{x}_{\text{par},k}$  :

$$\mathbf{x}_{\text{par},k} = \mathbf{x}_{\text{par},k-1} + \mathbf{v}_{\text{par},k-1} \quad (3)$$

$$\mathbf{y}_k = \mathbf{g}'(\mathbf{x}_k, \mathbf{x}_{\text{par},k}, \mathbf{n}_k) \quad (4)$$

3) *Joint estimation*: In joint estimation both the system state and the model parameters are estimated simultaneously. To this end, an augmented state vector is defined consisting of both the system state and the model parameters,  $\mathbf{x}_{\text{aug},k} = [\mathbf{x}_k^T, \mathbf{x}_{\text{par},k}^T]^T$ . Based on (1)–(4) a new state-space system is formed on which the filter is run.

4) *Dual estimation*: Similarly to joint estimation, in dual estimation the system state and the model parameters are estimated simultaneously. However, here the state system (1)–(2) and the parameter system (3)–(4) are kept separately, and two filters are run, one for the state estimation, and one for the parameter estimation. For each sample step  $k$  the result of the state estimation of the previous sample step  $\mathbf{x}_{k-1}$  is used as an input for the parameter estimator, and vice versa, the result of the parameter estimator of the previous sample step  $\mathbf{x}_{\text{par},k-1}$  is used in the state estimator as shown in Fig. 1.

In [2] it is suggested that the dual filter has better convergence properties than the joint filter.

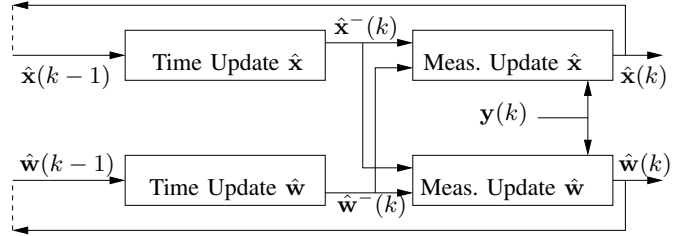


Fig. 1. The dual estimation scheme. The two filters use each other's estimation from the previous sample step.

### III. TRAFFIC MODEL

A widely used traffic flow model is the METANET model [13]. This model is suitable for filtering, since it captures the main dynamics of traffic flows, such as free-flow, congested flow, and the transitions between the two.

Below we present the basic equations of the METANET model, the boundary conditions, and the measurement equations, which will be used in the simulation experiments.

#### A. Basic METANET model

Consider a freeway link  $m$  that is subdivided into  $N_m$  segments, each with a length  $L_m$  and  $\lambda_m$  lanes, and a discrete time step with length  $T$  (h). Traffic dynamics is described in terms of the aggregated variables *speed*  $v_{m,i}(k)$  (km/h), *flow*  $q_{m,i}(k)$  (veh/h), and *density*  $\rho_{m,i}(k)$  (veh/km/lane), where  $i$  is the segment index.

The METANET model equations are given by the fundamental relationship between speed, density and flow

$$q_{m,i}(k) = \rho_{m,i}(k) v_{m,i}(k) \lambda_m, \quad (5)$$

the law of conservation of vehicles

$$\rho_{m,i}(k+1) = \rho_{m,i}(k) + \frac{T}{L_m \lambda_m} (q_{m,i-1}(k) - q_{m,i}(k)) + \xi_{m,i}^\rho(k) \quad (6)$$

and a heuristic relationship of the speed dynamics

$$v_{m,i}(k+1) = v_{m,i}(k) + \frac{T}{\tau} (V(\rho_{m,i}(k)) - v_{m,i}(k)) + \frac{T}{L_m} v_{m,i}^v(k) (v_{m,i-1}(k) - v_{m,i}(k)) - \frac{\eta T}{\tau L_m} \frac{\rho_{m,i+1}(k) - \rho_{m,i}(k)}{\rho_{m,i}(k) + \tilde{\kappa}} + \xi_{m,i}^v(k) \quad (7)$$

$$V(\rho_{m,i}(k)) = v_{\text{free},m} \exp \left[ -\frac{1}{a_m} \left( \frac{\rho_{m,i}(k)}{\rho_{\text{crit},m}} \right)^{a_m} \right] \quad (8)$$

where  $\xi_{m,i}^\rho(k)$ , and  $\xi_{m,i}^v(k)$  are random variables representing the random (unmodeled) dynamics in the speed and density evolution<sup>3</sup>. Furthermore,  $v_{\text{free},m}$  is the free-flow speed in segment  $m$ ,  $\rho_{\text{crit},m}$  is the critical density (the density at or above which traffic becomes unstable), and  $\tau$ ,  $\eta$ ,  $a_m$ ,  $\tilde{\kappa}$ , are model fitting parameters without direct physical meaning.

The model parameters are usually estimated off-line from measurement data. Their sensitivity is investigated numerically in [13] and the most sensitive parameters resulted to be  $v_{\text{free},m}$ ,  $\rho_{\text{crit},m}$  and  $a_m$ . These model parameters may change due to several external conditions such as weather conditions, percentage of trucks, light conditions, etc. This motivates the employment of dual or joint estimation algorithms for on-line simultaneous state and parameter estimation.

### B. Boundary conditions

The variables  $q_{m,0}$ ,  $v_{m,0}$ ,  $\rho_{m,N+1}$  are *boundary variables* which incorporate the influence of upstream and downstream segments from the considered link. Usually  $q_{m,0}$  and  $v_{m,0}$  can be measured directly, whereas in practice the density  $\rho_{m,N+1}$  is not measured directly and must be estimated. Even though  $q_{m,0}$  and  $v_{m,0}$  can be measured directly, the measurements will be corrupted by errors. Therefore we will consider all boundary variables as extra states of the system and we will estimate them from the measurement data, similarly to the other state variables. This approach is also recommended in [6]. The dynamic evolution of the boundary variables is described by a random walk:

$$\begin{bmatrix} q_{m,0}(k+1) \\ v_{m,0}(k+1) \\ \rho_{m,N+1}(k+1) \end{bmatrix} = \begin{bmatrix} q_{m,0}(k) \\ v_{m,0}(k) \\ \rho_{m,N+1}(k) \end{bmatrix} + \begin{bmatrix} \xi_{m,0}^q(k) \\ \xi_{m,0}^v(k) \\ \xi_{m,N+1}^\rho(k) \end{bmatrix} \quad (9)$$

where  $\xi_{m,0}^q(k)$ ,  $\xi_{m,0}^v(k)$ ,  $\xi_{m,N+1}^\rho(k)$  are stochastic variables.

### C. Measurements

The most frequently used traffic measurement devices typically measure speed and flow. For the segments that are equipped with sensors the measurement equations are:

$$y_{m,i}^q(k) = q_{m,i}(k) + n_{m,i}^q(k) \quad (10)$$

$$y_{m,i}^v(k) = v_{m,i}(k) + n_{m,i}^v(k) \quad (11)$$

where  $n_{m,i}^q(k)$ , and  $n_{m,i}^v(k)$  are the measurement noises for the flow and the speed respectively.

<sup>3</sup>Although (6) is an exact relationship and therefore modeling error is not present, we include the random variable  $\xi_{m,i}^\rho(k)$ , to allow a state filter to correct the number of vehicles in the network when it is wrongly initialized.

### D. State space representation

To bring equations (5)–(9) into the state-space representation required by the various filters, the state  $\mathbf{x}_k$  is defined as<sup>4</sup>  $\mathbf{x}_k = [\rho_1(k), \dots, \rho_N(k), v_1(k), \dots, v_N(k), v_0(k), q_0(k), \rho_{N+1}]^T$ , and the measurement vector  $\mathbf{y}_k$  collects the flow and speed measurements from (10) and (11) for the segments equipped with sensors.

## IV. SIMULATION SET-UP

In the simulations, the performances of the UKF and the EKF are compared for several filter configurations.

The link used in the simulations consists of four segments as shown in Fig. 2. The measurements are taken at the downstream end of a segment and consist of speed and flow. Several detector configurations are compared where the speed and flow detectors are placed at different locations.

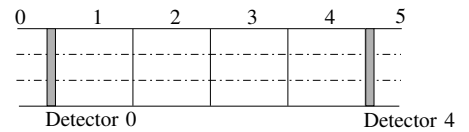


Fig. 2. The 4-segment link used for the simulations. Detectors may be placed at the boundaries of the segments.

For the evaluation of the different filter configurations artificial data was generated. The choice to use artificial data (opposed to real traffic data) was mainly motivated by the fact that for artificial data the real states and parameters are known, which allows for the evaluation of the filter performance. The data is generated by running the METANET model with a scenario in which the most important traffic phenomena are represented, such as traffic jams and upstream propagating waves, and free-flow with downstream propagating waves, and the transitions between congestion and free-flow. The scenario has a length of 3 hours and is shown for segment 3 in the Figures 3 and 4 by the dashed lines on the right.

To test the parameter tracking ability of the filters, the data was generated with the following time-varying parameters:

- the free-flow speed  $v_{\text{free},k}$  increases linearly from 119 km/h to 129 km/h,
- the critical density  $\rho_{\text{crit},k}$  varies sinusoidally around 27.4 veh/km/lane with an amplitude of 1 veh/km/lane,
- and  $a_k$ , decreases linearly from 2 to 1.7.

These values used for the generation of the data are shown in Fig. 3. The remaining parameters are given in Table III. The measurement noise standard deviations were chosen to be in the range of 5–10% of the typical values of the output variables, for the traffic state variables in the range of 1–5%, and the standard deviations of the parameters were tuned by trial and error. Note that the parameter covariances were used in the filters only, since for the data generations the parameters were predefined.

<sup>4</sup>The link index  $m$  is omitted in the rest of this section assuming that all the variables introduced hereafter refer to the same link.

TABLE III  
THE PARAMETERS USED.

$\text{cov}\{\xi_{m,i}^{\rho}(k)\} = 1 \text{ (veh/km/lane)}^2$
$\text{cov}\{\xi_{m,i}^v(k)\} = 1 \text{ (km/h)}^2$
$\text{cov}\{\xi^{\text{free}}\} = 10^{-2} \text{ (km/h)}^2$
$\text{cov}\{\xi^{\text{crit}}\} = 10^{-3} \text{ (veh/km/lane)}^2$
$\text{cov}\{\xi^a\} = 10^{-4} \text{ (-)}$
$\text{cov}\{n_{m,i}^v(k)\} = 10 \text{ (km/h)}^2$
$\text{cov}\{n_{m,i}^q\} = 100 \text{ (veh/h)}^2$
$\tau = 15.84 \text{ (s)}, \eta = 40 \text{ (km}^2\text{/h)}, \tilde{\kappa} = 5 \text{ (veh/km/lane)}$

To test the dependence of the state estimation performance on the parameters, the state estimator performance is compared for the case when the exact time-varying parameters are known and for the case when only a (constant) estimate of the parameters is available (which was taken to be the mean over the simulation period).

The performance measure defined for the state, parameter, dual, and joint estimators is chosen to be the root mean square relative error:

$$J_x = \sqrt{\frac{1}{n_x K} \sum_{j=1}^{n_x} \sum_{k=1}^K \frac{(\hat{\mathbf{x}}_{j,k} - \mathbf{x}_{j,k})^2}{\mathbf{x}_{j,k}^2}}$$

where the vector  $\hat{\mathbf{x}}_k$  is the quantity that is estimated (state, parameters, or both),  $\mathbf{x}_k$  is the real value,  $n_x$  is the dimension of  $\mathbf{x}_k$ , and  $K$  is the last sample index of the simulation.

In the simulation of the UKF, it may occur that the algorithm generates sigma points that are physically not meaningful, such as negative densities or negative free-flow speeds. To prevent this, upper and lower limits were imposed on both the states and parameters. The following limits were used, which were selected based on physical considerations:

$$\begin{aligned} 7 \text{ (km/h)} &\leq v_i(k) \leq 180 \text{ (km/h)}, \\ 0 \text{ (veh/km/lane)} &\leq \rho_i(k) \leq 180 \text{ (veh/km/lane)}, \\ 70 \text{ (km/h)} &\leq v_{\text{free}}(k) \leq 140 \text{ (km/h)}, \\ 20 \text{ (veh/km/lane)} &\leq \rho_{\text{crit}}(k) \leq 50 \text{ (veh/km/lane)}, \\ 1 &\leq a(k) \leq 3. \end{aligned}$$

The UKF design parameters were chosen as  $\kappa = 0, \alpha = 0.1$ .

## V. RESULTS

The results for the case when the speed and density are measured in all four segments are shown in Table IV. The performance of the EKF is comparable to that of the UKF (lower values indicate better performance). The errors of the joint configurations are significantly lower than those of the dual configuration. For other detector configurations, the results were similar (not shown here). These results are not in accordance with the suggestion in [2] that the dual filter should have better convergence properties. The reason for the worse performance of the dual filter could be the difference of a few orders of magnitude between the state covariances and the parameter covariances. Since the covariances of the states are much larger, the joint filter will in general adapt the state estimate more than the parameter estimate when a

TABLE IV  
THE PERFORMANCE OF THE EKF AND UKF FOR DIFFERENT FILTER TYPES WHEN ALL SEGMENTS ARE MEASURED.

filter type	estimation type	$J_{\rho}$	$J_v$	$J_{\text{par}}$
EKF	state	0.057	0.059	-
UKF	state	0.054	0.056	-
EKF	parameter	-	-	0.027
UKF	parameter	-	-	0.027
EKF	dual	0.206	0.160	0.233
UKF	dual	0.156	0.140	0.232
EKF	joint	0.054	0.055	0.35
UKF	joint	0.049	0.051	0.42

TABLE V  
THE PERFORMANCE OF THE EKF FOR THE STATE ESTIMATION PROBLEM KNOWN AND UNKNOWN TIME-VARYING PARAMETERS (ALL SEGMENTS ARE MEASURED).

time-varying parameters	$J_{\rho}$	$J_v$
known	0.052	0.053
unknown (average)	0.057	0.059

new measurement arrives. However, the dual filter will not balance the adaptation according to the covariances of the state and parameter estimates since the states are assumed to be given for the parameter estimator, and the parameters are given for the state estimator. See Figs. 3 and 4 for the estimated states and parameters by the joint and dual filters.

In Table VI, the effect of different detector locations on the performance is shown. As can be expected the estimated state shows larger error when fewer detectors are used. However, the parameter estimation error did not vary significantly with the number of detectors, except when only speed or density was measured at only one location. In the other cases, the performances of the EKF and the UKF are comparable.

The result for the state estimation with the EKF for the case when the time-varying parameters are exactly known, and the case when only the (constant) average is known, is shown in Table V. The small difference indicates that the state estimation filter is not very sensitive to parameter errors. This is in contrast with [6] where the result of the off-line

TABLE VI  
THE PERFORMANCE OF THE EKF AND UKF FOR DIFFERENT DETECTOR CONFIGURATIONS FOR JOINT ESTIMATION

filter type	flow loop locations	speed loop location	$J_{\rho}$	$J_v$	$J_{\text{par}}$
EKF	1,2,3,4	1,2,3,4	0.054	0.055	0.035
UKF	1,2,3,4	1,2,3,4	0.049	0.051	0.042
EKF	1,2,3	1,2,3	0.071	0.080	0.034
UKF	1,2,3	1,2,3	0.066	0.076	0.041
EKF	2,3	2,3	0.112	0.101	0.039
UKF	2,3	2,3	0.114	0.110	0.041
EKF	3	3	0.156	0.152	0.044
UKF	3	3	0.179	0.181	0.041
EKF	3	-	0.855	0.632	0.133
UKF	3	-	3.714	0.842	0.062
EKF	-	3	0.223	0.243	0.044
UKF	-	3	0.811	0.630	0.061

calibration was found to be sensitive to the model parameters. A possible reason for this is that the EKF re-estimates the state based on the new measurements (including model error/state noise, which can compensate for the parameter errors), while off-line calibration does not take model errors into account; it only minimizes the measurement error.

In general, it can be expected that the performance of the UKF is better than that of the EKF, since it propagates the state noise more accurately. In the results shown here, this is only weakly confirmed: the performances are nearly equal and in some cases the performance of the UKF is slightly better. A result that is not shown in the tables here, is that the UKF is dependent on the design parameters of the algorithm, and a change to  $\alpha = 1$  resulted in a slightly worse performance than that of the EKF.

## VI. CONCLUSION

Several filter configurations were investigated for freeway traffic state estimation, parameter estimation, and joint and dual estimation. The filters were tested with artificial data generated with the METANET traffic flow model. The main conclusions of the simulations are:

- Although the unscented Kalman filter has advantages that it propagates the state noise distribution with higher precision, its performance was nearly equal (slightly better) to that of the extended Kalman filter.
- The performance of the joint filter is better than that of the dual filter, because the joint filter takes into account the differences of the order of magnitude between the covariances of the states and the parameters.
- Fewer detectors result in larger state estimation errors, but have no effect on the parameter estimation error.

To broaden the validity of the results, in the future a wider range of scenarios and models will be considered, including on-ramp and off-ramp traffic, unknown turning rates in networks and the occurrence of incidents.

## ACKNOWLEDGMENTS

Research supported by the BSIK projects “Transition Sustainable Mobility (TRANSUMO)” and the Interactive Collaborative Information Systems (ICIS, grant no.: BSIK03024); and the Transport Research Centre Delft.

## REFERENCES

- [1] M. S. Grewal and A. P. Andrews, *Kalman Filtering*, T. Kailath, Ed. Prentice Hall, 1993, ISBN: 0-13-211335-X.
- [2] S. Haykin, Ed., *Kalman Filtering and Neural Networks*. Wiley & Sons, 2001.
- [3] S. Julier, J. Uhlmann, and H. Durrant-White, “A new method for nonlinear transformation of means and covariances in filters and estimators,” *IEEE Transactions on Automatic Control*, vol. 45, pp. 477–482, 2000.
- [4] E. A. Wan and R. van der Merwe, “The unscented Kalman filter for nonlinear estimation,” in *IEEE Symposium on Adaptive Systems for Signal Processing, Communication and Control*, 2000, pp. 153–158.
- [5] B. Ristic, S. Arulampalam, and N. Gordon, *Beyond the Kalman filter*. Artech House, 2004, ISBN: 1-58053-631.
- [6] Y. Wang and M. Papageorgiou, “Real-time freeway traffic state estimation based on extended Kalman filter: a general approach,” *Transportation Research Part B: Methodological*, vol. 39, no. 2, pp. 141–167, 2005.

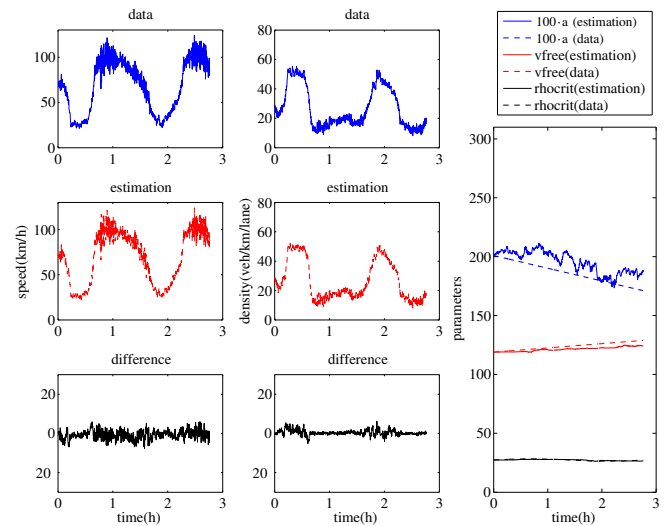


Fig. 3. State and parameter estimation with the joint EKF, all segments are measured.

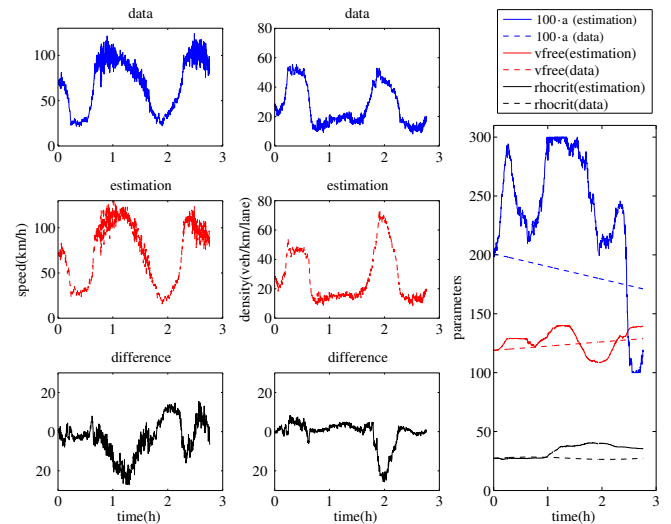


Fig. 4. State and parameter estimation with the dual EKF, all segments are measured.

- [7] A. T. Nelson, “Nonlinear estimation and modeling of noisy time-series by dual Kalman filtering methods,” Ph.D. dissertation, Oregon Graduate Institute, 2000.
- [8] Y. Wang and M. Papageorgiou, “An adaptive freeway traffic state estimator and its real-data testing—Part I: Basic properties,” in *Proceedings of the 8th International IEEE Conference on Intelligent Transportation Systems*, Vienna, Austria, Sept.13–16 2005, pp. 531–536.
- [9] —, “An adaptive freeway traffic state estimator and its real-data testing—Part II: Adaptive capabilities,” in *Proceedings of the 8th International IEEE Conference on Intelligent Transportation Systems*, Vienna, Austria, Sept.13–16 2005, pp. 537–548.
- [10] L. Mihaylova and R. Boel, “A particle filter for freeway traffic estimation,” in *Proceedings of the 43rd IEEE Conference on Decision and Control*, Atlantis, Paradise Island, Bahamas, 2004, pp. 2106–2111.
- [11] X. Sun, L. Munoz, and R. Horowitz, “Mixture Kalman filter based highway congestion mode and vehicle density estimator and its application,” in *Proceedings of the American Control Conference*, Boston, USA, 2004, pp. 2098–2103.
- [12] Y. Wang, M. Papageorgiou, and A. Messmer, “A real-time freeway network traffic surveillance tool,” *IEEE Transactions on Control Systems Technology*, vol. 14, no. 1, pp. 18–32, Jan. 2006.
- [13] M. Papageorgiou, J.-M. Blosseville, and H. Hadj-Salem, “Modelling and real-time control of traffic flow on the southern part of Boulevard

Périphérique in Paris: Part I: Modelling," *Transportation Research Part A*, vol. 24A, no. 5, pp. 345–359, 1990.